RSC Advances

Check for updates

Ni(II)-based coordination polymers for efficient electrocatalytic oxygen evolution reaction

Zhi-Qiang Jiang, *[a] Yu-Feng Li,[a] Xue-Jun Zhu,[a] Jin Lu,[a] Lei Zhang [b]
and Tian Wen *[b]

The exploration of highly efficient, stable and cheap water oxidation electrocatalysts using earth-abundant elements is still a great challenge. Herein, alkaline-stable cationic Ni(II) coordination polymers (Ni-CPs) were successfully obtained under hydrothermal conditions, which could stabilize the incorporation of Fe(III) to form Fe-immobilized Fe@Ni-CPs. The newly developed Ni-based CPs were used for the first time as an effective electrocatalyst for the oxygen evolution reaction in strong alkaline media.

The oxygen evolution reaction (OER) plays a vital role in energy storage and conversion applications due to energy issues and the need for sustainable development.[1-4] Because of the sluggish kinetics of the OER, excellent electrocatalysts are required to work in acidic or strong alkaline environments.[5,6] Noble metal-based catalysts like IrO_2 and RuO_2 with high efficiency showed excellent OER catalytic activity.[7] However, noble metal with high-cost and scarcity are impractical for scale-up applications. Currently, to substitute these precious metal-based materials, transition-metal-based (Fe, Co, Ni and so on) and metal-free (e.g., N, P and S) hybrid materials have been extensively developed.[8-10] For example, metal–organic frameworks (MOFs) such as ZIF-8/67 derived metal–carbon composite materials exhibit promising electrocatalytic performance.[11,12] Unfortunately, the pyrolysis process destroys the framework completely and causes agglomeration of metals, resulting in a decreased number of active sites. Therefore, to explore highly efficient and low-cost OER catalysts that can be directly used in the OER without calcination are desired, including complexes and MOFs.

Recently, much of transition bimetallic materials showed excellent electrocatalytic activity.[13-15] However, a handful of examples such as Fe–Co-MOFs or Co–Ni-MOFs have been explored due to instability, poor conductivity and harsh synthesis conditions.[16-20] Notably, the disadvantages of MOFs have limited their usage in the potential OER. Therefore, it is urgent to develop cheap, stable and active OER catalysts to replace the precious metals. However, this is still a great challenge. Coordination polymers (CPs) with a low-dimensional framework similar to MOFs are constructed by metal ion and organic ligands with potential active sites and functional groups, exhibiting wide applications in sensing, photoluminescence and photocatalysis.[21-26] However, rare examples of CPs have been directly explored in the OER. For Fe/Ni-based bimetal electrocatalysts, a novel strategy involves doping Fe(III) into a functional Ni-based CPs, which could enhance the electrocatalytic OER activities.

Herein, we report the hydrothermal synthesis of a Ni-based CPs as a high-performance OER electrocatalyst in strong alkaline solutions (Scheme 1). The blue crystals of $[Ni(bp)_3 \cdot (H_2O)_2] \cdot (bp) \cdot (ClO_4)_2$ (bp = 4,4′-biprydine) were obtained upon the reaction of bp ligands with $NiClO_4 \cdot 6H_2O$ under hydrothermal systems. Chemical stability tests displayed that **Ni-CPs** could retain their original framework in water or even a strong alkaline (pH = 14) solution after 12 hours (Fig. S1†), which is rarely reported for most transition metal CPs. The thermogravimetric analysis (TGA) showed that there is a significant change at about 110 °C due to the weight loss of the partial guest (Fig. S2†). Interestingly, the cationic **Ni-CPs** successfully captured the Mohr's salt (ammonium iron(II) sulfate) by taking advantage of the post-synthetic strategy. The obtained **Fe@Ni-CPs** exhibited a high-efficient OER activity under strong alkaline conditions.

Single-crystal X-ray diffraction analysis revealed that the **Ni-CPs** crystallized in the $C2/c$ space group (Table S1†). The obtained Ni coordination polymer was the isostructural

[a]Deep-processing of Fine Flake Graphite Sichuan Province Key Laboratory of Colleges and Universities, Panzhihua University, Panzhihua, Sichuan, 617000, P. R. China. E-mail: jiangzhiqiang@mail.pzhu.edu.cn

[b]School of Chemistry, The University of Melbourne, Parkville, Victoria 3010, Australia. E-mail: tian.wen@unimelb.edu.au

† Electronic supplementary information (ESI) available. CCDC [1858717]. For ESI and crystallographic data in CIF or other electronic format see DOI: 10.1039/c8ra07492e
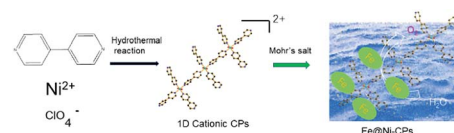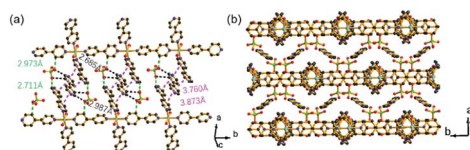

Scheme 1 Illustration of the synthesis process for Fe doped Ni coordination polymers for the OER.
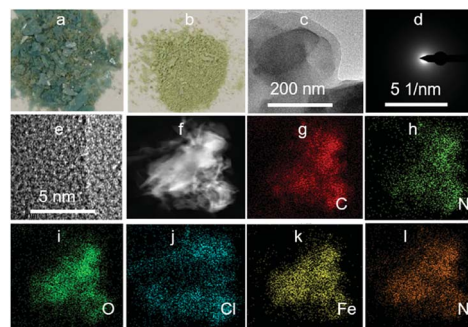
compound reported by Talham,[27] but their packing modes were distinctly different (Fig. S3–S5†). It also had a similar coordination environment to the railroad-like double chains synthesized by Yaghi.[28] The parallel chains were occupied by 4,4′-bpy, perchlorate and water molecules. In the **Ni-CPs**, most of the phenyl rings adopted the face-to-face mode. There were evident $\pi\cdots\pi$ interactions between the adjacent 4,4′-biprydine (Fig. 1a). In addition, there were strong intermolecular hydrogen bonds between 4,4′-bpy and perchlorate (strong Cl–O$\cdots$C amongst adjacent layers) (Fig. 1a). The weak reaction increased the high density of the framework and protected the coordination bonds against external guest attacking. These chains and guests were further packed with a three-dimensional structure along the c-axis (Fig. 1b).

The unique cationic Ni-CPs framework has the potential to immobilize some counterpart ions. To demonstrate this, Mohr's salts were investigated. Most strikingly, the color slowly changed from blue to green in an aqueous solution, given by the optical image (Fig. 2a and b), which not only indicated that Ni-CPs captured Mohr's salts via ion-exchange, but also suggested an alteration in the valence of Fe ions. It was possible that Fe^{2+} may have been further oxidized to Fe^{3+} under the O_2 and water environment when we prepared the Fe@Ni-CPs ($4Fe^{2+} + 2H_2O + O_2 = 4Fe^{3+} + 4OH^-$). The PXRD pattern showed that the frameworks remained unchanged after doping with Fe ions (Fig. S1†). From the transmission electron microscopy (TEM) images (Fig. 2c), after immobilization, the morphology of the **Fe@Ni-CPs** was still level and smooth; no ring-like patterns arose corresponding to the selected area for electron diffraction (SAED) (Fig. 2d), indicating that no bulk Fe particles formed during ion-exchange. This was further demonstrated using high resolution TEM (HRTEM) (Fig. 2e), in which there was no lattice fringe of crystallized Fe. The well distribution of C, N, O, Cl, Fe, and Ni in **Fe@Ni-CPs** was demonstrated by elemental mapping (Fig. 2f–l). Energy-dispersive X-ray spectroscopy (EDX) also agreed well with the above mapping data (Fig. S6†). In addition, the Fe^{3+} uptake was 4.1 wt%, as determined by inductively coupled plasma atomic emission spectroscopy (ICP). These results showed Fe ions to have been successfully immobilized by the **Ni-CPs**.

The X-ray photoelectron spectroscopy (XPS) survey spectrum of the **Fe@Ni-CPs** also showed the presence of C, N, O, Cl, Fe, and Ni elements (Fig. 3a). The Fe 2p high resolution XPS spectrum exhibited peaks at 725 eV and 711 eV (Fig. 3b), further indicating the presence of the Fe^{3+} oxidation state. This could
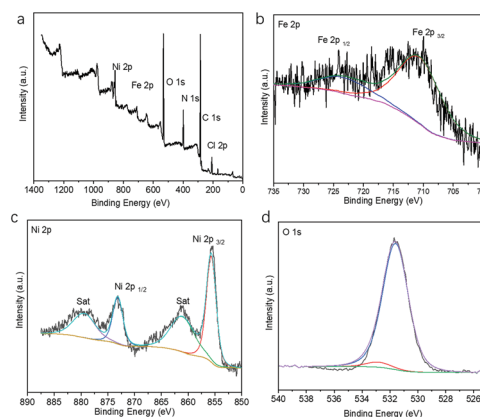

Fig. 2 (a–b) The optical image of Ni-CPs and Fe@Ni-CPs; (c) TEM images of Fe@ Ni-CPs; (d–e) the corresponding SAED and HRTEM pattern. (f–l) Element mapping of C, N, O, Cl, Fe, and Ni in Fe@Ni-CPs.

be explained by the transformations of Fe^{2+} to Fe^{3+} during the ion-exchange process. Similarly, in the Ni 2p spectra (Fig. 3c), two main peaks located at 855.8 eV and 873.5 eV can be ascribed to Ni^{2+} $2p_{3/2}$ and Ni^{2+} $2p_{1/2}$, respectively. These peaks are associated with two shakeup satellite peaks, indicating that Ni still remained in a divalent state. The Cl 2p and N 1s region could be corresponded to the ClO_4^- and biprydine, respectively (Fig. S7†). The O 1s spectrum (Fig. 3d) was divided into two peaks at 531.7 eV and 533.2 eV, which could be assigned to the OH group from filled H_2O molecules and partial ClO_4^-, respectively.

The above **Ni-CPs** with Fe doping encouraged us to investigate its electrocatalytic application in oxygen evolution reaction. To study the electrocatalytic activity of **Fe@Ni-CPs** for the OER, linear sweep voltammetry (LSV) was performed in a strong alkaline solution (pH = 14) for Fe@Ni-CPs@GC (fresh samples coated on glassy carbon electrode with Nafion binder). **Fe@Ni-CPs@GC** directly acted as working electrodes and showed good OER activity with an onset potential of 1.52 V (Fig. 4a), over-potential of 368 mV at 10 mA cm^{-2}, and a Tafel slope of 59.3 mV dec^{-1} (Fig. 4b). These OER performances are close to some reported MOFs catalysts (Table S2†) and even better than commercial benchmark OER catalysts like RuO_2 working at the same condition (Fig. S8†). In contrast, the electrocatalytic OER activities of the pristine **Ni-CPs@GC** without Fe incorporation

Fig. 1 (a) The weak reaction between chains in Ni CPs, showing the Cl–O$\cdots$C (green and black dashed line) and $\pi\cdots\pi$ interactions (pink dashed line) between the adjacent perchlorate and 4,4′-biprydine, respectively; (b) the packing view of Ni CPs along the c-axis. Cl in green, Ni in pale blue, N in blue, O in red and C in black. H atoms and partial guest molecules were omitted for clarity.

Fig. 3 (a) XPS survey spectrum of the Ni-CPs; XPS spectra of the Ni-CPs in the (b) Fe 2p, (c) Ni 2p, and (d) O 1s regions.
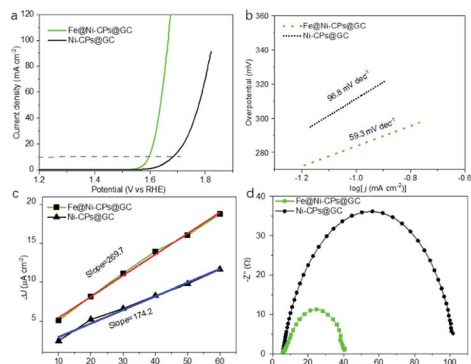
Fig. 4 (a) OER polarization curves and (b) Tafel plots of various electrocatalysts in a 1 M KOH aqueous solution; (c) linear relationship of the current density at 1.1 V (*vs.* RHE) *vs.* scan rates for Fe@Ni-CPs@GC and Ni-CPs@GC; (d) EIS of Fe@Ni-CPs and Ni-CPs electrode.

displayed much worse activity. The onset potential, overpotential (at 10 mA cm^{-2}), and the Tafel slope reached 1.62 V, 458 mV, and 96.8 mV dec^{-1}, respectively (Fig. 4a and b). In addition, **Fe@Ni-CPs** showed a strong durability during the OER process. The chronoamperometric response of **Fe@Ni-CPs** displayed a slight anodic current attenuation within 12 h due to the peeling of samples during the evolution of a large amount of O$_2$ gas (Fig. S9†). Furthermore, LSV of **Fe@Ni-CPs** showed negligible changes after OER tests for 12 h (Fig. S10†). These results indicate that the Fe-doped Ni-CPs with more active sites could serve as an excellent candidate for OER in strong alkaline conditions.

When Fe(III) was introduced, the resulting **Fe@Ni-CPs** catalysts greatly improved OER catalytic performance. There were dynamic collisions between Fe^{3+} ions and **Ni-CPs**, which allowed for more accessible catalytic active sites compared to the **Ni-CPs**. Particularly, Fe(III) doping can contribute to the adsorption and reaction of OH$^-$ groups in OER process.[29] As a result, **Fe@Ni-CPs** enhanced charge transfer under an apt electronic environment of the mixed Fe···Ni systems. In addition, electrochemical impedance spectrum and double-layer capacitance (C_{dl}) of the **Fe@Ni-CP** were also studied. The C_{dl} of **Fe@Ni-CPs** was confirmed to be 269.7 μF cm^{-2} (Fig. 4c and S11†), which is higher than that of **Ni-CPs** (C_{dl} = 174.2 μF cm^{-2}) (Fig. 4c and S12†). The semicircular diameter in EIS of **Fe@Ni-PCP** was smaller than that of **Ni-CPS** (Fig. 4d). These results further showed that **Fe@Ni-CPs** were more effective in enlarging the catalytically active surface area, conductivity and synergistic effects between Fe and Ni in comparison to Ni-CPs coated on electrodes.

In conclusion, a new alkaline-stable cationic Ni(II) coordinated polymers was synthesized under hydrothermal conditions. The Ni CPs could quickly interact with Mohr's salt. Interestingly, the Ni CPs could act as a unique oxidation matrix to realize the transformation of Fe^{2+} to Fe^{3+} during the ion-exchange process. Furthermore, the resulting **Fe@Ni-CPs** electrode, for the first time, showed an excellent electrocatalytic activity for OER in strong alkaline media. This study provides a new avenue to explore stable coordinated polymers by

incorporating the low-cost and high-activity transition metal, Fe, which will substitute the rare noble metals used in energy-related research.

Conflicts of interest

There are no conflicts to declare.

Acknowledgements

Notes and references

1 (a) M. Gräetzel, *Acc. Chem. Res.*, 1981, **14**, 376; (b) A. J. Bard and M. A. Fox, *Acc. Chem. Res.*, 1995, **28**, 141.
2 K. Maeda, K. Teramura, D. L. Lu, T. Takata, N. Saito, Y. Inoue and K. Domen, *Nature*, 2006, **440**, 295.
3 Y. Zhou, X. F. Guan, H. Zhou, K. Ramadoss, S. Adam, H. J. Liu, S. Lee, J. Shi, M. Tsuchiya, D. D. Fong and S. Ramanathan, *Nature*, 2016, **534**, 231.
4 B. Y. Xia, Y. Yan, N. Li, H. B. Wu, X. W. Lou and X. C. Wang, *Nat. Energy*, 2016, **1**, 15006.
5 A. Yin, J. M. Tan, C. Besson, Y. V. Geletii, D. G. Musaev, A. E. Kuznetsov, Z. Luo, K. I. Hardcastle and C. L. Hill, *Science*, 2010, **328**, 342.
6 Y. Jiao, Y. Zheng, M. Jaroniec and S. Z. Qiao, *Chem. Soc. Rev.*, 2015, **44**, 2060.
7 (a) C. C. L. McCrory, S. Jung, J. C. Peters and T. F. Jaramillo, *J. Am. Chem. Soc.*, 2013, **135**, 16977; (b) C. C. McCrory, S. Jung, I. M. Ferrer, S. M. Chatman, J. C. Peters and T. F. Jaramillo, *J. Am. Chem. Soc.*, 2015, **137**, 4347.
8 (a) H. Zhang, Z. Ma, J. Duan, H. Liu, G. Liu, T. Wang, K. Chang, M. Li, L. Shi, X. Meng, K. Wu, J. K. Ye, M. Li, L. Shi, X. Meng, K. Wu and J. Ye, *ACS Nano*, 2016, **10**, 684; (b) H. Zhang, Z. Ma, G. Liu, L. Shi, J. Tang, H. Pang, K. Wu, T. Takei, J. Zhang, Y. Yamauchi and J. Ye, *NPG Asia Mater.*, 2016, **8**, 293.
9 (a) Y. H. Qian, I. A. Khan and D. Zhao, *Small*, 2017, **13**, 1701143; (b) M. Jahan, Z. L. Liu and K. P. Loh, *Adv. Funct. Mater.*, 2013, **23**, 5363; (c) X. B. Liu, Y. C. Liu and L. Z. Fan, *J. Mater. Chem. A*, 2017, **5**, 15310; (d) Y. J. Tang, M. R. Gao, C. H. Liu, S. L. Li, H. L. Jiang, Y. Q. Lan, M. Han and S. H. Yu, *Angew. Chem., Int. Ed.*, 2015, **54**, 12928.
10 (a) S. Peng, L. Li, X. Han, W. Sun, M. Srinivasan, S. G. Mhaisalkar, F. Cheng, Q. Yan, J. Chen and S. Ramakrishna, *Angew. Chem., Int. Ed.*, 2014, **126**, 12802; (b) M. Li, T. Liu, X. Bo, M. Zhou, L. Guo and S. Guo, *Nano Energy*, 2017, **33**, 221; (c) S. Dong, X. Chen, X. Zhang and G. Cui, *Coord. Chem. Rev.*, 2013, **257**, 1946.
11 H. B. Zhang, J. W. Nai, L. Yu and X. W. Lou, *Joule*, 2017, **1**, 77.
12 (a) J. Yang, F. Zhang, H. Lu, X. Hong, H. Jiang, Y. Wu and Y. Li, *Angew. Chem., Int. Ed.*, 2015, **54**, 10889; (b) J. Yang,

F. Zhang, X. Wang, D. He, G. Wu, Q. Yang, X. Hong, Y. Wu and Y. Li, *Angew. Chem., Int. Ed.*, 2016, **55**, 12854; (*c*) Y. Chen, S. Ji, Y. Wang, J. Dong, W. Chen, Z. Li, R. Shen, L. Zheng, Z. Zhuang, D. Wang and Y. Li, *Angew. Chem., Int. Ed.*, 2017, **56**, 6937; (*d*) X. Wang, W. Chen, L. Zhang, T. Yao, W. Liu, Y. Lin, H. Ju, J. Dong, L. Zheng, W. Yan, X. Zheng, Z. Li, X. Wang, J. Yang, D. He, Y. Wang, Z. Deng, Y. Wu and Y. Li, *J. Am. Chem. Soc.*, 2017, **139**, 9419.

13 (*a*) J. Chi, H. M. Yu, B. W. Qin, L. Fu, J. Jia, B. L. Yi and Z. G. Shao, *ACS Appl. Mater. Interfaces*, 2017, **9**, 464; (*b*) Y. J. Tang, C. H. Liu, W. Huang, X. L. Wang, L. Z. Dong, S. L. Li and Y. Q. Lan, *ACS Appl. Mater. Interfaces*, 2017, **9**, 16977.

14 F. L. Li, Q. Shao, X. Q. Huang and J. P. Lang, *Angew. Chem., Int. Ed.*, 2018, **57**, 1888.

15 (*a*) J. M. Lv, D. X. Bai, L. Yang, Y. Guo, H. Yan and S. L Xu, *Chem. Commun.*, 2018, **54**, 8909; (*b*) D. Li, H. Baydoun, C. N. Verani and S. L. Brock, *J. Am. Chem. Soc.*, 2016, **138**, 4006.

16 J. Shen, P. Liao, D. Zhou, C. He, J. Wu, W. Zhang, J. Zhang and X. Chen, *J. Am. Chem. Soc.*, 2017, **139**, 1778.

17 S. L. Zhao, Y. Wang, J. C. Dong, C. T. He, H. J. Yin, P. F. An, K. Zhao, X. F. Zhang, C. Gao, L. J. Zhang, J. W. Lv, J. X. Wang, J. Q. Zhang, A. M. Khattak, N. A. Khan, Z. X. Wei, J. Zhang, S. Q. Liu, H. J. Zhao and Z. Y. Tang, *Nat. Energy*, 2016, **1**, 16184.

18 J. Duan, S. Chen and C. Zhao, *Nat. Commun.*, 2017, **8**, 15341.

19 (*a*) C. W. Kung, J. E. Mondloch, T. C. Wang, W. Bury, W. Hoffeditz, B. M. Klahr, R. C. Klet, M. J. Pellin, O. K. Farha and J. T. Hupp, *ACS Appl. Mater. Interfaces*, 2015, **7**, 28223; (*b*) L. Wang, Y. Z. Wu, R. Cao, L. T. Ren, M. X. Chen, X. Feng, J. W. Zhou and B. Wang, *ACS Appl. Mater. Interfaces*, 2016, **8**, 16736; (*c*) K. Maity, K. Bhunia, D. Pradhan and K. Biradha, *ACS Appl. Mater. Interfaces*, 2017, **9**, 37548.

20 J. Xing, K. Guo, Z. Zou, M. Cai, J. Du and C. Xu, *Chem. Commun.*, 2018, **54**, 7046.

21 Z. Hu, B. J. Deibert and J. Li, *Chem. Soc. Rev.*, 2014, **43**, 5815.

22 Y. J. Cui, Y. F. Yue, G. D. Qian and B. L. Chen, *Chem. Rev.*, 2012, **112**, 1126.

23 M. O'Keeffe, M. A. Peskov, S. J. Ramsden and O. M. Yaghi, *Acc. Chem. Res.*, 2008, **41**, 1782.

24 Q. L. Zhu and Q. Xu, *Chem. Soc. Rev.*, 2014, **43**, 5468.

25 M. Albrecht, M. Lutz, A. L. Spek and G. van Koten, *Nature*, 2000, **406**, 970.

26 T. Wen, D. Zhang, J. Liu, R. Lin and J. Zhang, *Chem. Commun.*, 2013, **49**, 5660.

27 J. D. Woodward, R. Backov, K. A. Abboud, H. Ohnuki, M. W. Meisel and D. R. Talham, *Polyhedron*, 2003, **22**, 2821.

28 O. M. Yaghi, H. l. Li and T. L. Groy, *Inorg. Chem.*, 1997, **36**, 4292.

29 Y. Zheng, Y. Jiao, Y. Zhu, Q. Cai, A. Vasileff, L. H. Li, Y. Chen, Y. Han and S. Z. Qiao, *J. Am. Chem. Soc.*, 2017, **139**, 3336.